Field-induced transition in the layered manganite $LaEu_{0.2}Sr_{1.8}Mn_2O_7$

2001 J. Phys.: Condens. Matter 13 917

(http://iopscience.iop.org/0953-8984/13/5/311)

INSTITUTE OF PHYSICS PUBLISHING JOURNAL OF PHYSICS: CONDENSED MATTER

J. Phys.: Condens. Matter **13** (2001) 917–927 www.iop.org/Journals/cm PII: S0953-8984(01)16934-1

Field-induced transition in the layered manganite $LaEu_{0.2}Sr_{1.8}Mn_2O_7$

Jun Zhang[1], **Qiwei Yan, Fangwei Wang, Peng Yuan and Panlin Zhang**

State Key Laboratory for Magnetism, Institute of Physics and Centre for Condensed Matter Physics, Chinese Academy of Sciences, Beijing 100080, People's Republic of China

E-mail: zhang32@sanken.osaka-u.ac.jp (Jun Zhang)

Received 7 September 2000, in final form 28 November 2000

Abstract

We report on the effect of substitution of Eu on the structure, magnetic and transport properties of the layered manganese oxides $La_{1.2-x}Eu_xSr_{1.8}Mn_2O_7$ ($x = 0$–0.4). With Eu substituting for some of the La, the MnO_6 octahedron shows an anomalous lattice distortion, especially in the case of $x = 0.2$. Eu substitution suppresses the ferromagnetic (FM) metallic state, resulting in a FM cluster-glass state for $x \leqslant 0.2$ and no magnetic ordering for $x > 0.2$. $LaEu_{0.2}Sr_{1.8}Mn_2O_7$ ($x = 0.2$) undergoes a metamagnetic transition from the proposed layered FM cluster-glass state to the long-range FM state under a 4 T field, as well as a magnetic-field-induced insulating–metallic transition. The relationships among the lattice effect, exchange interactions and magnetotransport properties are discussed.

1. Introduction

Observations of a colossal-magnetoresistance (CMR) effect have reanimated extensive research interest in the manganese oxides with perovskite structure [1–3], $R_{1-x}M_xMnO_3$ (R is a rare-earth element and M is an alkaline-earth metal). Properly substituting M^{2+} for R^{3+} can cause ferromagnetic (FM) and metallic states instead of the antiferromagnetic (AFM) and insulating states in the undoped $RMnO_3$, and a dramatic decrease of resistivity around T_C under application of a magnetic field, i.e. a CMR effect. These properties can be understood in the light of the double-exchange (DE) interaction mechanism [4, 5] by considering the electron hopping between Mn^{3+}/Mn^{4+} ions through a Mn–O–Mn network, as well as the charge–lattice coupling effect resulting from Jahn–Teller (JT) distortion [6, 7]. The most important parameters controlling the properties of the perovskite oxides are the doping concentration x and the ion sizes at (R, M) sites. The former controls the band filling of the one-electron e_g band and the kinetic energy of charge carriers, and the latter acts as a chemical pressure, which results in

[1] Author to whom any correspondence should be addressed. Present address: Institute of Scientific and Industrial Research, Osaka University, 8-1 Mihogaoka, Ibaraki, Osaka, 567-0047, Japan. Telephone: 81-06-6879-4140; fax: 81-06-6879-4140.

0953-8984/01/050917+11$30.00

lattice distortion and modifies the transfer integral t of the e_g electron and the bandwidth of the e_g band.

Besides the well-known ABO_3-type manganese oxides with perovskite structure, the manganese oxides with layered perovskite structure (see figure 1), $R_{2-2x}M_{1+2x}Mn_2O_7$, also show the CMR effect [8–11]. Due to the intrinsic layered and quasi-two-dimensional structure, the layered manganites exhibit some anomalous phenomena different from those shown by the ABO_3-type oxides and have become the focus of recent studies concerned with the CMR effect. The strong anisotropy of exchange interactions in the layered manganites makes it possible to investigate the relationship between the local spin correlation and the corresponding magnetotransport behaviour. The competition between the FM DE interaction and the AFM super-exchange interaction is found to be a key factor controlling the properties of the layered oxides. Tuning the concentration and size of the rare-earth ion R^{3+} could lead the competition to a delicate balance, and give rise to some complex magnetic structures, such as spin canting and spin glass, and novel properties. Detailed research on $La_{1.2-x}Nd_xSr_{1.8}Mn_2O_7$ polycrystals [12, 13] has shown that the properties can be chemically controlled, and continuously changed by substituting Nd for La. Moritomo *et al* [14, 15] have found that Nd doping changes the ground states of $La_{2-2x}Sr_{1+2x}Mn_2O_7$ ($x = 0.3$ and 0.4), and the application of a magnetic field induces a transition from an AFM or paramagnetic (PM) state to a FM one. Herein, we replace

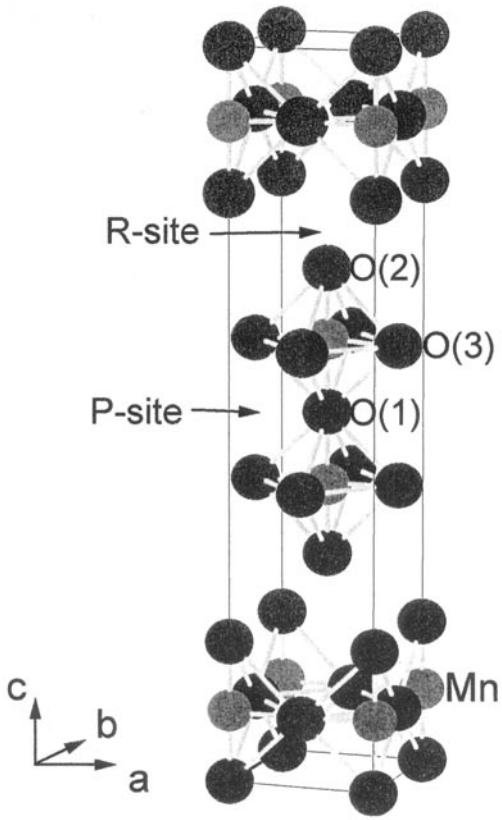

Figure 1. The schematic crystal structure of the layered perovskite $(R, M)_3Mn_2O_7$. Dark circles are O atoms; light circles are Mn atoms; (R, M) atoms which are located among the MnO_6 octahedra are not shown.

La^{3+} in $La_{1.2}Sr_{1.8}Mn_2O_7$ by Eu^{3+}, which has a much smaller ionic radius and larger magnetic moment than Nd^{3+}; therefore we obtain a much stronger lattice distortion and a more severe influence on the Mn spin array. So in the Eu-substituted system, some distinct properties can be expected, and a clear and exact correlation between structural parameters and properties may be derived. In fact, we have found an anomalous lattice distortion and field-induced transitions in $LaEu_{0.2}Sr_{1.8}Mn_2O_7$. The relationships among the lattice distortion, exchange interactions and properties are discussed.

2. Experiment

Bulk samples of $La_{1.2-x}Eu_xSr_{1.8}Mn_2O_7$ ($x = 0$–0.4) were prepared by a standard solid-state reaction. Stoichiometric amounts of La_2O_3, Eu_2O_3, $SrCO_3$, $MnCO_3$ were mixed, ground and calcined at 1000 °C for 24 h in air. The powders were well ground again, then pelletized and sintered at 1250 °C for 48 h with an intermediate grinding. The samples were characterized by x-ray diffraction (XRD) on a Rigaku diffractometer using Cu Kα radiation, and the step-scanning XRD data were collected to refine the crystal structure using the Rietveld program. Magnetization measurements were carried out using a SQUID magnetometer (Quantum Design), and resistivities ρ were measured by the standard four-probe method.

3. Results and discussion

The XRD measurements show that all prepared samples of $La_{1.2-x}Eu_xSr_{1.8}Mn_2O_7$ are of single phase with $Sr_3Ti_2O_7$-type tetragonal structure ($I4/mmm$). The results of the Rietveld refinement of the XRD data including the cell parameters and the atom sites of the Mn and O, as well as the calculated Mn–O bond lengths, are listed in table 1. With smaller Eu^{3+} being substituted for La^{3+}, the cell parameters a and c decrease, showing a lattice contraction. It is notable that Eu substitution results in an anomalous lattice distortion, and unsymmetrical changes of the Mn–O bond length in the MnO_6 octahedron are observed. As shown in figure 1, in a MnO_6 octahedron, there are three different O atom sites, O(1), O(2) and O(3), and, correspondingly, three types of Mn–O bond, i.e. the apical Mn–O(1) bond inside the double-perovskite layer, the apical Mn–O(2) bond near the rock-salt layer (between the bilayers, not

Table 1. Results of the Rietveld structure refinement (lattice parameters and atom sites) and the calculated Mn–O bond lengths for $La_{1.2-x}Eu_xSr_{1.8}Mn_2O_7$ ($x = 0$–0.4).

Compound:	$La_{1.2}$	$La_{1.1}Eu_{0.1}$	$La_{1.0}Eu_{0.2}$	$La_{0.9}Eu_{0.3}$	$La_{0.8}Eu_{0.4}$
x	0	0.1	0.2	0.3	0.4
a (Å)	3.8714(3)	3.8677(2)	3.8653(1)	3.8614(2)	3.8572(3)
c (Å)	20.097(2)	20.072(1)	20.076(2)	20.038(1)	20.022(1)
Mn	(0, 0, 0.0994)	(0, 0, 0.0994)	(0, 0, 0.0975)	(0, 0, 0.0990)	(0, 0, 0.0989)
O(1)	(0, 0, 0)	(0, 0, 0)	(0, 0, 0)	(0, 0, 0)	(0, 0, 0)
O(2)	(0, 0, 0.1952)	(0, 0, 0.1990)	(0, 0, 0.1971)	(0, 0, 0.2014)	(0, 0, 0.2029)
O(3)	(0, 0.5, 0.0958)	(0, 0.5, 0.0949)	(0, 0.5, 0.0963)	(0, 0.5, 0.0951)	(0, 0.5, 0.0952)
d_{Mn-O1} (Å)	1.998	1.995	1.957	1.984	1.980
d_{Mn-O2} (Å)	1.925	1.999	2.000	2.052	2.082
d_{Mn-O3} (Å)	1.937	1.936	1.933	1.932	1.930
Δ	1.01	1.03	1.02	1.04	1.05
R_{wp}	13.49	12.22	7.41	11.64	12.43

shown in figure 1) and the equatorial Mn–O(3) bond. With x increasing from 0 to 0.4, the Mn–O(1) and four Mn–O(3) bonds contract slightly, but only the Mn–O(2) bond obviously elongates (table 1), which results in an increase of $\Delta = d_{\mathrm{Mn-O(apical)}}/d_{\mathrm{Mn-O(equator)}}$ ($d_{\mathrm{Mn-O(apical)}}$ is the average apical Mn–O bond length, $d_{\mathrm{Mn-O(equator)}}$ is the equatorial Mn–O(3) bond length), showing an enhancement of the JT distortion.

The anomalous changes of the Mn–O bond length with Eu doping resemble those observed under pressure [16], indicating the comparability of the effects of chemical pressure and hydrostatic pressure. For the chemical pressure effect observed here, the selective occupation of (R, M) ions should be considered. There are two different sites for (R, M) ions: the twelve-coordination site within the perovskite bilayers (P site) and the nine-coordination site in the rock-salt layers between the perovskite bilayers (R site) (figure 1). The Rietveld refinements reveal that, as Eu^{3+} replaces La^{3+}, the smaller Eu^{3+} preferentially occupies the smaller R sites, and more Sr^{2+} occupies the larger P sites, resulting in a decrease of the average ion size of the R site, tension in R sites and compression in P sites, which is favourable for lengthening of the Mn–O(2) bond and contraction of the other bonds. In addition, compared with other bonds, the Mn–O(2) bond is free from the confinement by Mn–O–Mn linkage and, therefore, is free to adjust to retain the mean Mn–O bond length according to the valence-bond sum rule.

Among these $La_{1.2-x}Eu_xSr_{1.8}Mn_2O_7$ samples, the $x = 0.2$ compound shows a lattice distortion which is a special case. As x increases from 0 to 0.4, the general trend of structure distortion is for the Mn–O(1) bond to shorten slightly and the Mn–O(2) bond to extend remarkably. But the opposite variation is observed for $x = 0.2$. As x increases from 0.1 to 0.2, both Mn and O(2) atoms move in the intralayer direction (nearer to O(1)); this results in a significant reduction in the Mn–O(1) bond length but no change in the Mn–O(2) bond length, releasing the JT distortion (decreasing Δ); and at the same time, the lattice constant c increases, with the result that the distance between bilayers increases. The anomalous lattice distortion in $La_{1.2-x}Eu_xSr_{1.8}Mn_2O_7$ will have an effect on the exchange interactions and the magnetotransport properties of the layered manganites, especially for the special case of the $x = 0.2$ compound, $LaEu_{0.2}Sr_{1.8}Mn_2O_7$. We also noticed that at a certain doping level, the Eu-doped system shows a much larger lattice distortion than the Nd-doped system [22] due to Eu^{3+} being smaller than Nd^{3+}, so the influence of Eu doping on the properties should be more drastic.

Now we turn to the magnetic and transport properties of $La_{1.2-x}Eu_xSr_{1.8}Mn_2O_7$. Figure 2 shows the temperature dependence of the magnetization measured at 0.1 T for all of the samples with $x = 0$–0.4. The results for the undoped sample, $La_{1.2}Sr_{1.8}Mn_2O_7$, are in agreement with the previous reports [8, 13, 17], with the FM Curie temperature T_C and the short-range or two-dimensional (2D) magnetic ordering temperature T^* about 120 K and 245 K, respectively. Eu doping suppresses the ferromagnetism significantly and the result is magnetic frustration and disorder. For $x = 0.1$, T_C and T^* decrease to 70 and 220 K, respectively. With decrease in temperature, the magnetization increases steeply below 80 K, shows a maximum at 30 K and then decreases gradually, indicating the onset of magnetic disorder. The obvious discrepancy between the zero-field-cooled (ZFC) and field-cooled (FC) magnetizations below 30 K further suggests the presence of disordered spins frozen in a cluster-glass state at low temperature [18]. The $x = 0.2$ sample also shows a characteristic FM cluster-glass state, with much lower magnetization, indicating that the FM ordering becomes much weaker. The detectable increase of the magnetization at $T^* \sim 200$ K originates from the 2D FM order, and the large increase below $\sim$60 K should be attributed to the formation and growth of FM clusters. Besides the 2D FM order, another possible origin of the small steps in the magnetization observed near 150–250 K for these samples is intergrowth in the layered oxides. As x increases to 0.3 and 0.4, the magnetization behaviour resembles those of $La_{1.2-x}Nd_xSr_{1.8}Mn_2O_7$ ($x = 0.8$) [13]

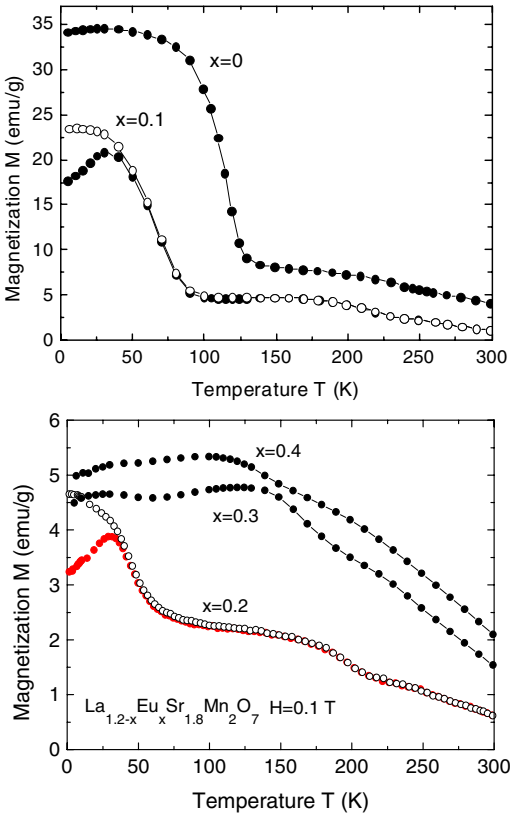

Figure 2. The temperature dependence of the magnetization for $La_{1.2-x}Eu_xSr_{1.8}Mn_2O_7$ (x = 0–0.4) at 0.1 T. The open circles denote the FC data.

and $Ln_{1.4}Sr_{1.6}Mn_2O_7$ (Ln = Pr and Nd) [19], with no sign of long-range magnetic ordering, confirming that Eu doping has a stronger influence on FM ordering than Nd doping.

The field-dependent magnetization curves at 5 K are shown in figure 3 for all samples. The undoped sample ($x = 0$) shows a strong FM feature, with a saturation moment of about 3 μ_B which is a little lower than the theoretical value 3.6 μ_B as the spins are fully aligned in parallel. When x increases to 0.1, the spontaneous magnetization decreases, which should be attributed to the presence of the low-temperature cluster-glass state. But at higher fields (>0.5 T) the magnetization increases gradually up to near the saturation value for the $x = 0$ sample at 6 T, reflecting the fact that the spin disorder between FM clusters can be suppressed by a magnetic field. For $x = 0.3$ and 0.4, no spontaneous magnetization is observed, and the magnetization value increases linearly and slowly with field >1 T, with no saturation tendency even at 6 T, showing the characteristics of spin disorder. More attention should be concentrated on the $x = 0.2$ sample, which shows a special magnetization behaviour. Below 3 T, the magnetization feature for $x = 0.2$ is almost identical to those for $x = 0.3$ and 0.4. At 4 T, the magnetization increases abruptly, doubling within a narrow field range of 0.4 T, and then reaches saturation. Before and after this jump, the magnetization curve for $x = 0.2$ coincides with those for $x = 0.3$ and 0.4 and that for $x = 0$, respectively, indicating that the jump of magnetization results from a magnetic-field-induced transition from spin disorder to FM order.

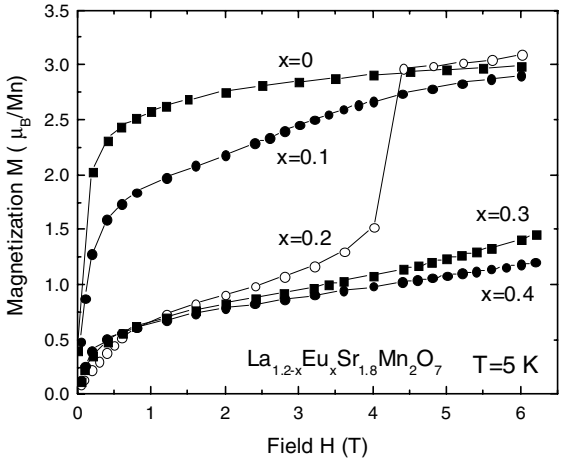

Figure 3. The field dependence of the magnetization for $La_{1.2-x}Eu_xSr_{1.8}Mn_2O_7$ ($x = 0$–0.4) at 5 K.

Similar transitions had ever been observed in the Nd-doped series of the layered oxides $La_{1.2-x}Nd_xSr_{1.8}Mn_2O_7$ [13, 14] and $(La_{1-z}Nd_z)_{1.4}Sr_{1.6}Mn_2O_7$ [15], but some differences still exist. For the Nd-doped series, the transition occurs in a wide range of doping concentration, but for the Eu-doped samples, only for $x = 0.2$. In addition, a sharp transition that occurs only for the single crystals of the Nd-doped series is observed here in the Eu-doped polycrystalline sample. For $(La_{1-z}Nd_z)_{1.4}Sr_{1.6}Mn_2O_7$ single crystals [15], the transition is ascribed to that from AFM to FM order. However, for $LaEu_{0.2}Sr_{1.8}Mn_2O_7$, no direct proof of AFM order can be obtained from our experimental results, although we cannot eliminate the possibility of the presence of short-range AFM fluctuation. It has been found that an A-type AFM state does occur in the layered perovskites [15, 20]. In this magnetic structure, the FM bilayer alternates along the *c*-axis, i.e. the AFM super-exchange interaction overwhelms FM double-exchange interaction between bilayers. As a result of the competition between these two opposite exchange interactions, spin canting, fluctuation and disorder, as well as the simple FM and AFM order, could come into being along the interlayer direction, depending on the relative strength of the two exchange interactions. The metamagnetic transition observed here in $LaEu_{0.2}Sr_{1.8}Mn_2O_7$ should be attributed to the field suppression of spin disorder between the FM clusters, which extend along the *ab*-plane and probably consist of several (or more) FM bilayers. This magnetic structure model will be discussed further below.

The field-induced metamagnetic transition is strongly temperature dependent. Figure 4 plots the magnetization curves at different temperatures for $LaEu_{0.2}Sr_{1.8}Mn_2O_7$, as well as the corresponding reverse magnetization curves measured as the field is decreased. At 5 K, the reverse magnetization curve shows typical FM characteristics. The irreversibility of the magnetization behaviour excludes the possibility that the jumping of the magnetization originates from a quantum effect, and confirms the first-order nature of the field-induced transition. At 10 K, the increase of the magnetization becomes a continuous process and extends through a wider field range from 2.5 T to 5 T. The field necessary for producing the transition decreases from 4 T at 5 K to 2.5 T at 10 K, indicating that higher temperature makes it easier for the spins of FM clusters to rotate under an applied field. But at 40 K, the magnetization increases almost linearly with field below 4 T and then tends to saturate, and the reverse magnetization curve almost duplicates the normal one. It is believed that the frozen

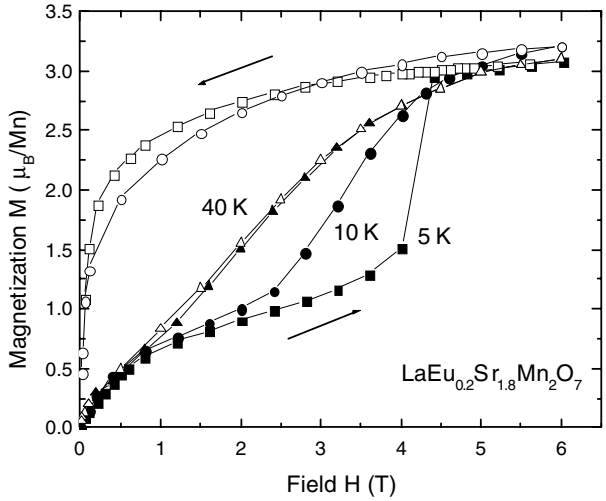

Figure 4. Magnetization (solid symbols) and reverse magnetization (open symbols) curves for $LaEu_{0.2}Sr_{1.8}Mn_2O_7$ at different temperatures.

FM clusters are melted at 40 K, resulting in the transition disappearing, which further confirms that the field-induced transition is related to the FM cluster-glass state. The strong temperature dependence of the transition suggests that the FM cluster-glass state is not stable and can be modified by outside disturbances such as changes in temperature and magnetic field.

The magnetotransport properties of $La_{1.2-x}Eu_xSr_{1.8}Mn_2O_7$ ($x = 0$–0.3) are shown in figure 5. The undoped sample, $La_{1.2}Sr_{1.8}Mn_2O_7$ ($x = 0$), shows an insulating–metallic (I–M) transition at $T_{IM} \sim 125$ K near T_C. Under a 6 T field, the resistivity decreases obviously and T_{IM} shifts to higher temperature, resulting in a large MR effect with the MR peak at around T_{IM} and a considerable low-temperature MR effect below 100 K. With Eu replacing La, the resistivity increases and the transport behaviour changes greatly, especially when $x > 0.1$. For $x = 0.1$, T_{IM} decreases to 80 K, but below 30 K the resistivity increases again on cooling, showing an insulating–metallic–insulating (I–M–I) transition. The re-emergence of the insulating behaviour is in accord with the decrease of the ZFC magnetization below 30 K (see figure 2), and should be related to the magnetic frustration and carrier localization due to the low-temperature cluster-glass state. Although the re-entrant insulating behaviour is still present at 6 T, a large MR effect is observed over a wide temperature range below 100 K with no MR peak. When $x > 0.1$, insulating behaviours are observed over the whole temperature range of the measurements without an applied field. It is notable that under 6 T, an I–M transition is induced at 75 K when $x = 0.2$, although insulating behaviour re-emerges below 25 K. The I–M–I transition for $x = 0.2$ at 6 T resembles that for $x = 0.1$ at zero field, indicating that the application of a field alters the transport behaviour for $x = 0.2$ making it similar to that for $x = 0.1$, just like the case for the corresponding change of the magnetization behaviour. Due to the field-induced I–M transition, the resistivity decreases by two to three orders of magnitude at low temperature, giving rise to an enormous low-temperature MR effect below 50 K, with the largest MR ratio $(\rho_0 - \rho_H)/\rho_0$: up to 99.8%. However, for $x = 0.3$ and 0.4 (only the data for $x = 0.3$ are shown), no I–M transition takes place even under a field of 6 T, but the enhancement of the low-temperature MR effect is still evident. Compared with the Nd doping [13], Eu doping is more effective in destroying the metallic state of $La_{1.2}Sr_{1.8}Mn_2O_7$, consistently with the doping effect on magnetic properties shown above.

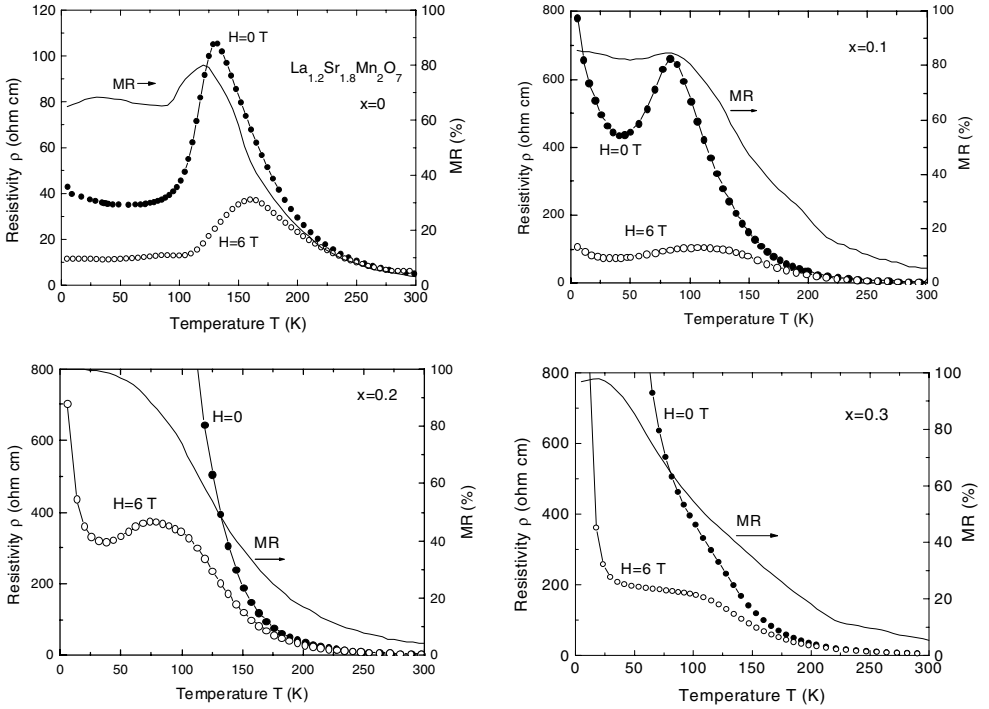

Figure 5. Resistivities at zero field and 6 T, and the resultant MR ratio, as functions of temperature for $La_{1.2-x}Eu_xSr_{1.8}Mn_2O_7$ ($x = 0$–0.3).

The field-induced I–M transition in $LaEu_{0.2}Sr_{1.8}Mn_2O_7$ ($x = 0.2$) should be attributed to the metamagnetic transition from a FM cluster-glass state to FM state mentioned above. Figure 6 shows the field dependence of the resistivity for $LaEu_{0.2}Sr_{1.8}Mn_2O_7$, which shows some correlation with the field dependence of the magnetization (see figure 4). At 5 K, with field increasing, the resistivity shows a two-step decrease. The decreases in resistivity below 0.5 T and between 2 and 4 T are related to the increase in magnetization below 1 T and at 4 T, respectively, although the change in the resistivity seems to be somewhat ahead of that of the magnetization. Above 4 T, where the magnetization tends to saturation, the resistivity becomes insensitive to the field. However, at 30 K the resistivity decreases steeply below 1 T, above which the resistivity remains almost unchanged, giving rise to a large low-field MR ratio: ∼90% at 1 T. So the resistive transition should have its origin in the magnetic transition. Accompanying the magnetic transition from the cluster-glass state to the FM state, the spin scattering of carriers undergoes a reduction, resulting in the abrupt decrease of the resistivity and the I–M transition.

The magnetic and transport properties described above show that the ferromagnetic and metallic state of $La_{1.2-x}Eu_xSr_{1.8}Mn_2O_7$ is suppressed and then destroyed upon La being replaced by Eu. The structure refinement results described above have revealed an anomalous distortion of the MnO_6 octahedron in $La_{1.2-x}Eu_xSr_{1.8}Mn_2O_7$. Eu doping elongates the apical Mn–O bond and enhances the JT distortion, which will stabilize the $d_{3z^2-r^2}$ orbital of the e_g electron as compared with the $d_{x^2-y^2}$ orbital and reduce the transfer integral t of the e_g electron, resulting in the FM state being suppressed [16]. The increasing of the Mn–O(2) bond length weakens the interlayer exchange interaction. In addition, the large magnetic moments of the

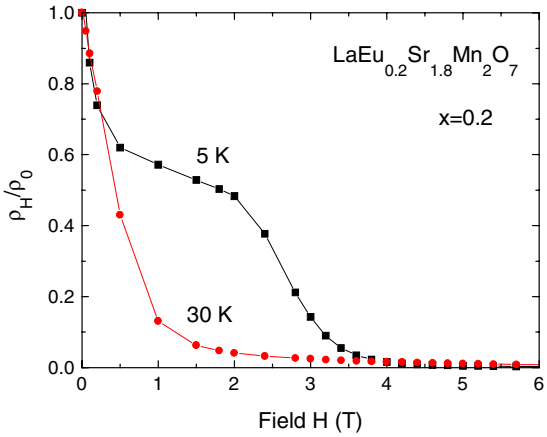

Figure 6. The field dependence of the normalized resistivity for $LaEu_{0.2}Sr_{1.8}Mn_2O_7$ at 5 K and 30 K.

doped Eu^{3+} will also interfere with the long-range FM ordering of Mn ion spins, especially along the interlayer direction where the exchange interaction between Mn ions is weaker. Due to Eu^{3+} having a much smaller ionic radius (and, therefore, larger lattice distortion) and larger magnetic moments than Nd^{3+}, both of these effects are stronger in the Eu-doped system than in the Nd-doped system previously reported on [12–15], and the suppression of the FM order is more significant in the former. Therefore, different magnetic structure could be expected for the Eu-doped system. Considering the above analysis and the layered structure of the oxides, we suppose that layered FM clusters may come into being in the $x = 0.2$ compound at low temperature. Due to the lattice effect and the influence of Eu^{3+} moments, the competition between the AFM exchange interaction and the FM exchange interaction results in the collapse of interlayer FM ordering and spin fluctuation, spin canting and even AFM ordering between some perovskite bilayers. Although the interlayer long-range FM ordering is destroyed, the FM ordering inside the layers probably still persists, forming special layered FM clusters. The short-range FM ordering inside the clusters is the origin of the weak ferromagnetism. An important characteristic of the layered FM cluster model is that the spin disorder exists only along the interlayer direction, with AFM fluctuation between some clusters. This is somewhat similar to the A-type AFM structure, which is dominant in some layered perovskites. Under an applied field, the disordered state is suppressed, and the antiparallel clusters begin to rotate, with the angle between them decreasing. When the applied field is high enough to overcome a critical energy barrier, i.e. the AFM exchange interaction between the clusters, the angle decreases to below 90°. Then the spins tend to align in parallel at once under such a large field, and the FM order at the cluster boundaries is immediately enhanced so as to restore the long-range FM order, resulting in the observed transition from the FM clusters (short-range FM order) to the long-range FM order (figure 3). But with temperature increasing, the clusters frozen in the glass state start to melt, and the canted AFM order is destroyed, so as the field increases the moments rotate gradually and the magnetization increases continuously. However, for both cases—abrupt and continuous increases—the applied field would suppress the spin canting and disorder, enhance the three-dimensional (long-range) FM ordering and, correspondingly, reduce the localization of carriers, resulting in a sudden drop of the resistivity, the insulating–metallic transition and a large MR effect. In addition, considering the supposed layered FM cluster structure, the observed large MR effect probably has a contribution from

the spin-valve-type MR [15]. Recently, a strong correlation between lattice striction and CMR was found for Pr-substituted $La_{1.2}Sr_{1.8}Mn_2O_7$ single crystals [21], similar to our Eu-doped system, and this has also been attributed to the e_g electron orbital degrees of freedom.

For the $x = 0.1$ compound, although the FM cluster-glass state also exists, the FM metallic state is fairly strong. The large magnetization (figures 2 and 3) implies that the FM clusters are of large size, and the spin fluctuation and disorder are of less consequence. But for $x = 0.3$ and 0.4, there is no cluster-type FM ordering. In these three compounds, no field-induced transition is observed. The confinement of the field-induced transition to the $x = 0.2$ case suggests that the $x = 0.2$ compound is near the boundary of a phase transition from the FM metallic state ($x = 0$–0.1) to the non-FM insulating ($x = 0.3$–0.4) state, and (i) a delicate equilibrium between the competitive FM and AFM coupling and (ii) a resulting suitable magnetic structure (i.e. a critical size of the FM clusters) are necessary for the transition to occur. The lattice distortion in the $x = 0.2$ compound is also very different from others. As mentioned before, on x increasing from 0.1 to 0.2, the Mn–O(1) bond contracts dramatically and the JT distortion becomes weaker (Δ decreases), but the distance between bilayers increases, which will strengthen the intralayer DE interaction and weaken the interlayer interaction, enhancing the anisotropy of the exchange interaction. This special lattice distortion and the resultant variation of the exchange interactions are beneficial to the formation of layered FM clusters, especially those with AFM fluctuation between them, which should be closely related to the field-induced transition being confined to just this compound. The strong effects of Eu doping in $La_{1.2-x}Eu_xSr_{1.8}Mn_2O_7$ reported here indicate that in the layered perovskite, the chemical pressure can modify the structure, exchange interactions and magnetotransport properties more effectively than in the ABO_3-type perovskites.

4. Conclusions

Eu substitution for La in $La_{1.2-x}Eu_xSr_{1.8}Mn_2O_7$ greatly suppresses the FM metallic state, and results in there being a FM cluster-glass state when $x = 0.1$ and 0.2 and no magnetic order when $x = 0.3$ and 0.4. For the $x = 0.2$ sample, we observed a magnetic-field-induced metamagnetic transition from the FM cluster-glass state to the long-range FM state and the I–M transition. These phenomena are related to the anomalous lattice distortion derived from chemical pressure and the influence of the Eu^{3+} magnetic moment on Mn local spins, both of which weaken FM exchange interactions and destroy the three-dimensional FM ordering. Compared with the Nd doping case, the larger lattice distortion and Eu^{3+} magnetic moment make the Eu doping effect more significant and distinctive. A model of a layered FM cluster structure with spin disorder and AFM fluctuation is proposed for interpreting the field-induced transition. That the transition is confined just to the $x = 0.2$ sample and the special lattice distortion in the $x = 0.2$ sample indicate that in the layered manganites, there is strong coupling among the lattice distortion, exchange interactions and other properties, and the competition between the different exchange interactions can be modified by chemical pressure and reach a subtle balance.

References

[1] Kusters R M, Singleton J, Keen D A, McGreevy R and Hayes W 1989 *Physica* B **155** 362
[2] Von Helmolt R, Wecker J, Holzapfel B, Schultz L and Samwer K 1993 *Phys. Rev. Lett.* **71** 2331
[3] Jin S, Tiefel T H, McCormack M, Fastnacht R A, Ramesh A and Chen L H 1994 *Science* **364** 413
[4] Zener C 1951 *Phys. Rev.* **82** 403
[5] de Gennes P-G 1960 *Phys. Rev.* **118** 141

[6] Millis A J, Shraiman B I and Mueller R 1996 *Phys. Rev. Lett.* **77** 175
[7] Roder H, Zang J and Bishop A R 1996 *Phys. Rev. Lett.* **76** 1356
[8] Moritomo Y, Asamitsu A, Kuwahara H and Tokura Y 1996 *Nature* **380** 141
[9] Kimura T, Tomioka Y, Kuwahara H, Asamitsu A, Tamura M and Tokura Y 1996 *Science* **274** 1698
[10] Asano H, Hayakawa J and Matsui M 1996 *Appl. Phys. Lett.* **68** 3638
[11] Battle P D, Green M A, Laskey N S, Millburn J E, Murphy L, Rosseinsky M J, Sullivan S P and Vente J F 1997 *Chem. Mater.* **9** 552
[12] Zhang J, Wang F, Zhang P and Yan Q 1999 *Solid State Commun.* **109** 401
[13] Zhang J, Wang F, Zhang P and Yan Q 1999 *J. Phys.: Condens. Matter* **11** 2413
[14] Moritomo Y, Maruyama Y, Akimoto T and Nakamura A 1997 *Phys. Rev.* B **56** R7057
[15] Moritomo Y and Itoh M 1999 *Phys. Rev.* B **59** 8789
[16] Argyriou D N, Mitchell J F, Goodenough J B, Chmaissem O, Short S and Jorgensen J D 1997 *Phys. Rev. Lett.* **78** 1568
[17] Argyriou D N, Mitchell J F, Potter C D, Bader S D, Kleb R and Jorgensen J D 1997 *Phys. Rev.* B **55** R11 965
[18] Mukherjee S, Ranganathan R, Anilkumar P S and Joy P A 1996 *Phys. Rev.* B **54** 9267
[19] Hur N H, Kim J T, Yoo K H, Park Y K, Park J C, Chi E O and Kwon Y U 1998 *Phys. Rev.* B **57** 10 740
[20] Moritomo Y, Maruyama Y, Akimoto T and Nakamura A 1998 *J. Phys. Soc. Japan* **67** 405
[21] Ogasawara H, Matsukawa M, Hatakeyama S, Yoshizawa M, Apostu M, Suryanarayanan R, Dhalenne G, Revcolevschi A, Itoh K and Kobayashi N 2000 *J. Phys. Soc. Japan* **69** 1274
[22] Zhang Jun *et al* unpublished data